Electro-Optical Properties of Polymers Containing Alternating Nonlinear Optical Chromophores and Bulky Spacers

Yi Liao,* Cyrus A. Anderson, Philip A. Sullivan, Andrew J. P. Akelaitis, Bruce H. Robinson, and Larry R. Dalton

Department of Chemistry, University of Washington, Seattle, Washington 98195

Received November 4, 2005. Revised Manuscript Received December 15, 2005

Alternating polymers of a nonlinear optical chromophore and bulky spacers were synthesized. High chromophore loading and efficient site isolation were achieved with this approach. The effects of chromophore loading density and electric poling field on the electro-optical (EO) properties of the polymers were carefully compared with those of guest−host systems of the same chromophore. The alternating polymer can be poled to higher EO efficiency under a lower poling field than the optimized guest−host system, while the λ_{max} of the polymer film is about 40 nm shorter than that of the guest−host system.

Introduction

Organic and polymeric nonlinear optical (NLO) materials have emerged as viable alternatives to conventional inorganic crystalline materials such as lithium niobate in electro-optical (EO) devices. Broad bandwidth[1] and low driving voltages[2] have been demonstrated by devices incorporating such material. High EO efficiency requires a highly ordered noncentrosymmetric alignment. Among many approaches generating highly ordered noncentrosymmetric alignment of NLO chromophores, electric field poling is the most widely studied method. Theoretical and experimental studies suggest that chromophore dipolar interaction, aggregation, shape effects, and so forth are important factors affecting poling efficiency.[3] As a result of these interactions between chromophores, any given system will have an optimum loading density. Increasing chromophore concentration past this optimum value will decrease the EO efficiency. Excellent agreement between theory and experimental data has been demonstrated for guest−host systems.[4]

Compared to guest−host systems, chromophore polymers have better homogeneity and stability. Polymers and dendrimers of NLO chromophores with well-designed architecture have shown very high EO efficiency.[5] Some of the values are much higher than those of guest−host systems employing similar active material. These results are interesting because they imply that local unisotropic order exists in these systems and the maximum EO efficiency predicted by the isotropic model[6] can be exceeded. Here, we report synthesis and EO properties of the alternating polymer **P1** and **P2** as well as the chromophore **1** for comparison. In the polymer structures, chromophores are separated by bulky dendrons or perfluorobenzenes. Polymers with dendronized chromophores and randomly grafted dendrons and chromophores have been studied and show large EO efficiency.[7] Compared with this previous work, the alternating structures of **P1** and **P2** ensure the site isolation of the chromophores, consequently avoiding chromophore aggregation even at high loading density. Our purpose in utilizing this design is to increase the optimum loading density and, hence, the EO efficiency.

Results and Discussions

Synthesis of the Polymers P1 and P2 and the chromophore 1. The target polymers **P1** and **P2** were synthesized by first polymerizing a dialcohol chromophore bridge **2** with a bulky dicarboxyl spacer **3** or **4** and then coupling the subsequent polymer with an electron acceptor to complete the active material (Scheme 1). Previous literature has shown that the benzyl ether dendritic architecture can provide strong steric interchromophore site-isolation effects,[8] while fluorinated polymers normally have good thermal stability and low optical loss. Therefore, **3** and **4** were chosen as the bulky spacers. Polymerization of the spacer unit with the chromophore bridge, rather than the complete chromophore, was necessary to avoid decomposition of the chromophore under the polymerization conditions. Compound **5**, the precursor of **3**, was synthesized from a straightforward nucleophilic substitution of 5-hydroxy-isophthalic acid dimethyl ester on

* To whom correspondence should be addressed. E-mail: liaoyi@u.washington.edu.

(1) Lee, M.; Katz, H. E.; Erben, C.; Gill, D. M.; Gopalan, P.; Heber, J. D.; McGee, D. J. *Science* **2002**, *298*, 1401.
(2) Shi, Y.; Zhang, C.; Zhang, H.; Bechtel, J. H.; Dalton, L. R.; Robinson, B. H.; Steier, W. H. *Science* **2000**, *288*, 119−122.
(3) Dalton, L. R. *Pure Appl. Chem.* **2004**, *76*, 1421−1433.
(4) Robinson, B. H.; Dalton, L. R. *J. Phys. Chem. A* **2000**, *104*, 4785−4795.
(5) For recent examples: Bai, Y.; Song, N.; Gao, J- P.; Sun, X.; Wang, X.; Yu, G.; Wang, Z.-Y. *J. Am. Chem. Soc.* **2005**, *127*, 2060. Huang, D.; Parker, T.; Guan, H.-W.; Cong, S.; Jin, D.; Dinu, R.; Chen, B.; Tolstedt, D.; Wolf, N.; Condon, S. *Proc. SPIE* **2005**, *5634*, 172. Luo, J.; Haller, M.; Ma, H.; Liu, S.; Kim, T.-D.; Tian, Y.; Chen, B.; Jang, S.-H.; Dalton, L. R.; Jen, A. K.-Y. *J. Phys. Chem. B* **2004**, *108*, 8523.
(6) Pereverzev, Y. V.; Prezhdo, O. V.; Dalton, L. R. *Chem. Phys. Chem.* **2004**, *5*, 1821.
(7) Luo, J.; Haller, M.; Li, H.; Tang, H.-Z.; Jen, A. K.-Y.; Jakka, K.; Chou, C.-H.; Shu, C.-F. *Macromolecules* **2004**, *37*, 248. Luo, J.; Liu, S.; Haller, M.; Liu, L.; Ma, H.; Jen, A. K.-Y. *Adv. Mater.* **2002**, *14*, 1763.
(8) Hecht, S.; Fréchet, J. M. J. *Angew. Chem., Int Ed.* **2001**, *40*, 75.

10.1021/cm0524392 CCC: $33.50
Published on Web 01/28/2006

1,3-bis-benzyloxy-5-bromomethyl-benzene using potassium carbonate as the base. Basic hydrolysis of **5** yielded **3**. The less massive perfluorobenzene based spacer **4** was utilized to further increase the loading density of the chromophore. Starting with a similar nucleophilic substitution, **6** was afforded by reacting 5-hydroxy-isophthalic acid dimethyl ester with 1-bromomethyl-2,3,4,5,6-pentafluoro-benzene. The methyl ester **6** was hydrolyzed under basic conditions affording **4**. Mass spectrometry, ^{1}H, and ^{13}C NMR suggest that the basic hydrolysis of **6** in methanol led to the replacement of the para-fluorine with a methoxy group. Proton decoupled ^{13}C NMR showing two doublets with coupling constants of 244 Hz supported that the substitution occurred at the para postion. Similar reaction occurring with pentafluorotoluene has been reported.[9] The chromophore bridge **2** was synthesized by acidic deprotection of **7**, which was synthesized by procedures similar to those in the literature.[10] Polymerizations via acid chloride and DCC/DMAP reactions were not successful partially because of the low solubility of the starting materials. Consequently, the experimental polymerization condition was adopted as the literature suggested that compounds featuring similar functional groups could be successfully copolymerized.[11] Pyridine, the solvent used in the polymerization steps, can dissolve both starting materials well. Compound **2** was polymerized with either **3** or **4**, by activating the carboxyl groups with tosyl chloride and *N*-piperidinoformamide in pyridine, yielding polymer backbones **P3** and **P4**, respectively. The alternating polymer systems **P1** and **P2** were completed by coupling the strong CF_3PhTCF acceptor[12] to **P3** and **P4**, respectively, via Knoevenagel condensation in ethanol. No aldehyde residue peak was observed in the NMR of **P1** and **P2**. Similarly, **1** was synthesized from **7** by a Knoevenagel reaction.

Site-Isolation Effects and Thermal Properties. The alternating structures of **P1** and **P2** ensure that every chromophore is surrounded by bulky dendrons or perfluorobezenes. Therefore, effective site isolation can be achieved to reduce chromophore aggregation even at high loading density. The site-isolation effect of the polymers was studied by UV−vis spectroscopy (Table 1). In tetrahydrofuran (THF) solution, polymers **P1** and **P2** have about the same λ_{max} as the chromophore **1**, which is consistent with the fact that they have the same active structures. In chloroform, λ_{max} of **1** increases 71 nm as a result of the solvatochromic effect, while the λ_{max} values of **P1** and **P2** shift only 9 and 6 nm, respectively. The highly reduced solvatochromic shifts can be explained by shielding of the chromophore via the bulky groups in the alternating polymer. More effectively shielded chromophores exhibit smaller changes in λ_{max} as shielded molecules are less affected by the solvent change. Such a strong site-isolation effect has been observed in some related

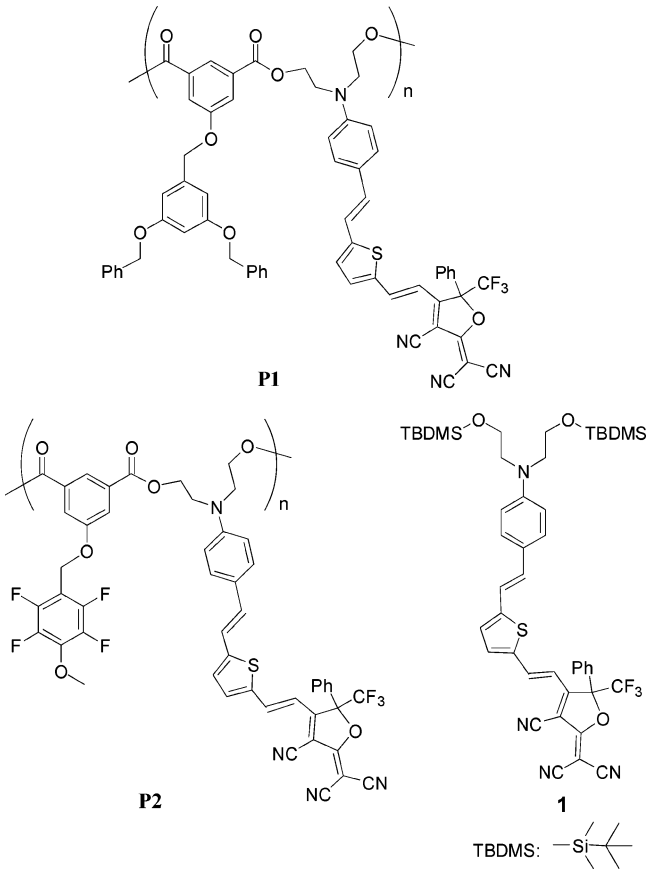

chromophore−dendrimer systems.[8] **P2**, with smaller bulky groups between the chromophores, exhibits a slightly stronger site-isolation effect than that of **P1** which has bigger dendrons. This may be due to a stronger interaction between the tetrafluoromethoxy benzene and the chromophore in **P2**. Compared to a film of 25% of **1** in amorphous polycarbonate [APC, poly(bisphenol A carbonate-*co*-4,4′-(3,3,5-trimethylcyclohexylidene)diphenol carbonate, Aldrich co.], films of **P1** and **P2** also have 33 and 39 nm lower λ_{max} values, respectively, which is a valuable property for reducing optical loss.

The glass-transition temperatures T_g of **P1** and **P2** were measured by differential scanning calorimetry (DSC). Although flexible dendrons tend to reduce T_g,[13] **P1** has a moderate T_g of 130 °C and **P2** has a higher T_g of 140 °C. This may be partially due to a stronger interaction between the tetrafluoromethoxy benzene and the chromophore as suggested by solvatochromism study.

EO Properties of Guest−Host System and Polymers. Though many NLO polymers have been studied in the past decade, few systematic comparisons with the corresponding guest−host systems have been reported. The EO efficiency of a guest−host system depends on the chromophore loading density. Maximum EO efficiency can only be achieved at an optimum loading density. The EO property of the polymers shall be compared to that of the guest−host system with optimum loading density. Therefore, we poled a series of guest−host samples with different loading densities of **1**

(9) Filler, R.; Ayyangar, N. R.; Gustowski, W.; Kang, H. H. *J. Org. Chem.* **1969**, *34*, 534.
(10) Rao, V. P.; Jen, A. K.-Y.; Wong, K. Y.; Droit, K. J. *Tetrahedron Lett.* **1993**, *34* (11), 1747.
(11) Higashi, F.; Haramoto, S.; Yashio, M. *Macromol. Chem. Phys.* **2002**, *203*, 309.
(12) Liao, Y.; Eichenger, B.; Firestone, K.; Haller, M.; Luo, J.; Kaminsky, W.; Benedict, J.; Reid, P.; Jen, A. K.-Y.; Dalton, L. R.; Robinson, B. *J. Am. Chem. Soc.* **2004**, *127*, 2758.
(13) For example: Chen, Y.-M.; Liu, Y.-F.; Gao, J.-G.; Chen, C.-F.; Xi, F. *Macromol. Chem. Phys.* **1999**, *200*, 2240.

Scheme 1. Synthesis of P1, P2, and 1

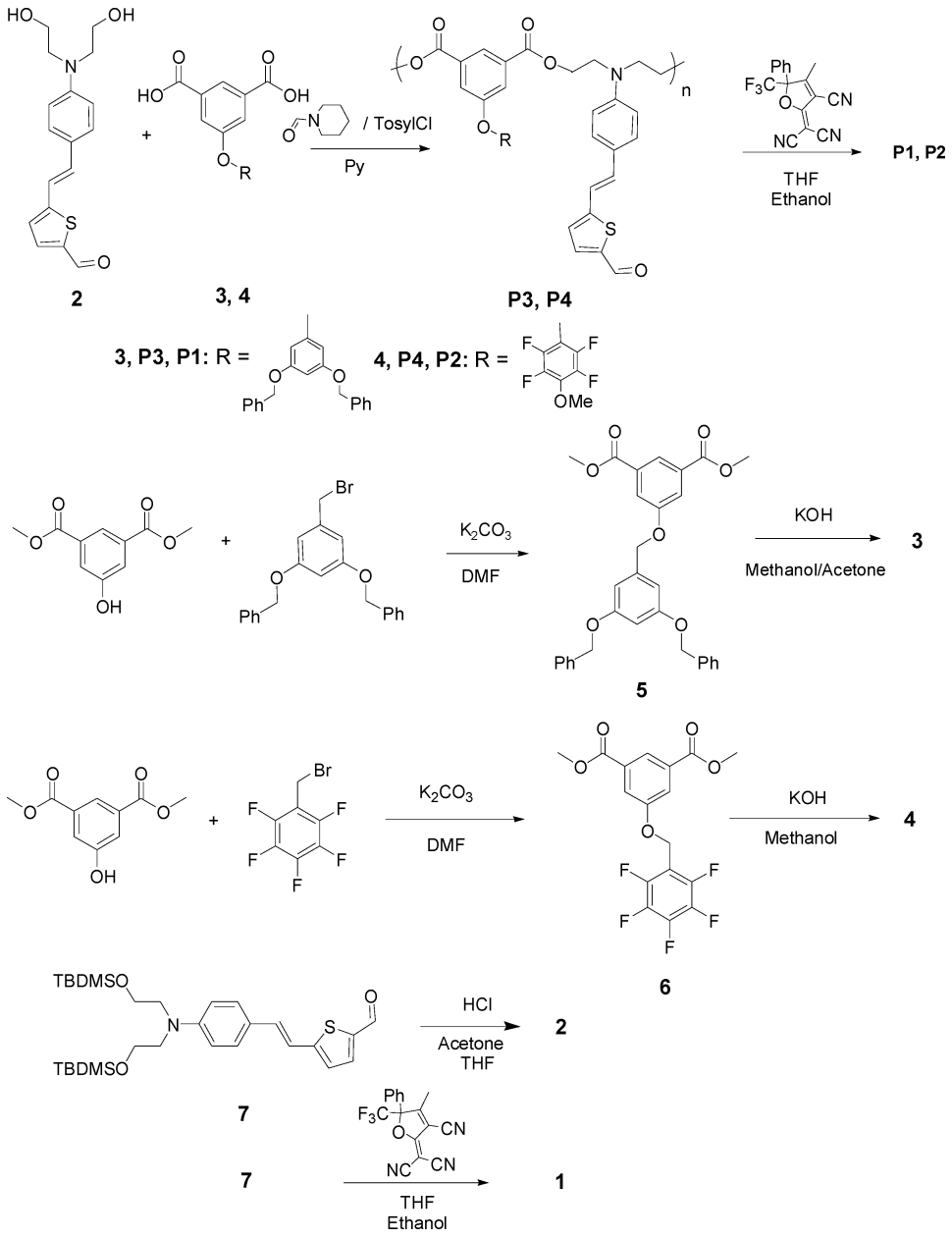

Table 1. λ_{max} (nm) of P1, P2, and 1

	P1	P2	1		P1	P2	1
THF	682	684	683	film	701	695	734[a]
$CHCl_3$	691	690	754				

[a] λ_{max} of a film of 25% **1** in APC.

in APC and measured the EO efficiency, r_{33}, by the simple refection method.[14] The electric field applied was around 115 MV/m. The highest temperature reached during the poling process depended on the loading density. As a result of the plasticizing effect of the doped chromophore, T_g is lowered with increased loading density. Therefore, the poling temperatures were adjusted correspondingly. Further increasing temperature or poling field resulted sample breakdown or electrode damage. The poling conditions and the results are listed in Table 2 and plotted in Figure 1. This study showed

(14) Teng, C.; Man, H. *Apply. Phys. Lett.* **1990**, *56*, 1734.

Table 2. Poling Conditions and r_{33} Values of the Guest−Host Systems with Different Loading Densities

loading density (wt %)	electric field (MV/m)	temperature (°C)	r_{33} (pm/V)[a]
15	120	145	35
25	115	135	52
30	115	125	50
38	115	115	40

[a] r_{33} was measured at 1300 nm.

that the optimum loading density is about 25%. At this loading density, a guest−host system can achieve 52 pm/V at 1300 nm. Higher loading density decreases the EO efficiency. Theoretically, this can be explained by strong dipolar interactions between the chromophores that were against the poling field. Furthermore, high loading density decreases T_g and increases conductivity, which decreases the poling voltage and temperature that can be applied. Samples with the 25 wt % loading were used for comparing optical and EO properties of the polymers.

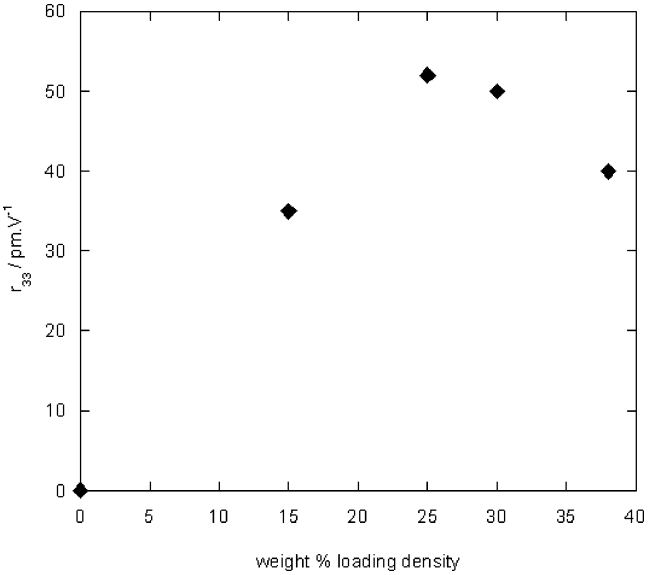

Figure 1. r_{33} of the guest−host systems with different loading densities.

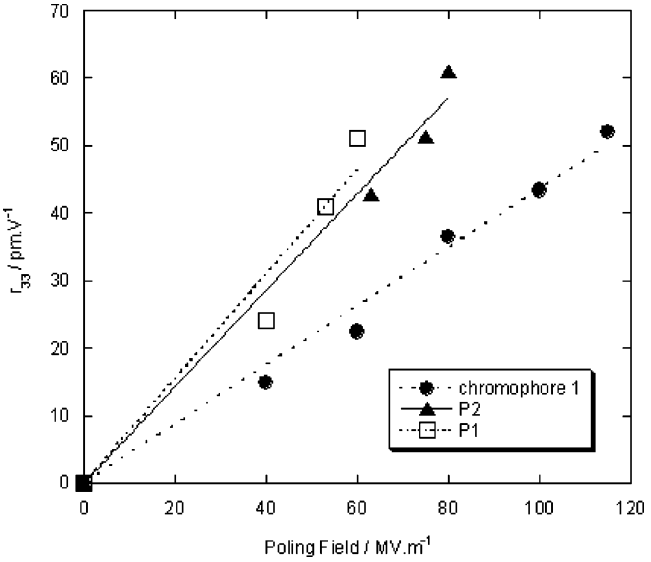

Figure 2. Field-dependent r_{33} of **P1**, **P2**, and **1**.

Given that **P1** and **P2** have T_g values of 130 and 140 °C, they were poled under similar conditions as the guest−host system. The resultant r_{33} values were in the range of 50−60 pm/V, which is similar to that of the guest−host system. We noticed that the current during the poling process was quite high compared with that of the guest−host systems. This high current limited the maximum poling field that could be applied to the film. The real voltage applied to the sample was directly measured from the two electrodes on the polymer films. Corresponding to a temperature dependent decrease in the inherent resistivity of the polymer films at optimum poling temperature, this voltage was shown to be much lower than the power supply setting. We found that, at 115 °C, the highest fields that can be applied to **P1** and **P2** were about 60 MV/m and 80 MV/m, respectively. Further increasing the power only increased current instead of field. Our recent research showed that high loading systems were generally much more conductive than the typical guest−host system with a loading density lower than 30 wt %. In this case, the enhanced conductivity may also be in part caused by unreacted terminal carboxylic acids. For 25% doped APC samples, the real poling voltage was close to the reading on the power supply.

Polymers **P1** and **P2** were poled under different potentials at 150 °C to evaluate the poling efficiency and the optimum EO efficiency. **P1** can achieve an r_{33} of 51 pm/V at 60 MV/m, while **P2** showed an r_{33} of 63 pm/V at 80 MV/m. No apparent decrease of EO efficiency was observed in several weeks at room temperature. The field-dependent r_{33} values of **P1** and **P2**, as well as 25 wt % doped APC samples, are plotted in Figure 2. On the basis of the assumption that r_{33} is directly proportional to the poling field E, the data were fit into a linear function, $r_{33} = kE$. The poling efficiency was evaluated by comparing the slope k of the three sets of data. The slope of the guest−host system of **1**, k_1, is 0.44 pm/V^2, while those of **P1** and **P2** are $k_{\mathbf{P1}} = 0.77$ pm/V^2 and $k_{\mathbf{P2}} = 0.71$ pm/V^2. These results showed that the poling efficiency of the polymer films is much higher than that of the optimized guest−host system. Therefore, similar r_{33} values can be achieved under moderate poling field, which may result in advantages in device fabrication.

Although the poling efficiencies of the polymers are much higher than that of the guest−host system, the ordering parameter of the grafted chromophore is actually lower. The number loading densities of **P1** and **P2** are 0.92 and 1.0 mmol/g and are more than three times higher than the number loading density of a 25 wt % guest−host system of **1** (0.3 mmol/g). The poling efficiencies of the polymer films are a little less than twice that of the guest−host film, which means the ordering parameter of the guest−host system is higher than that of the polymers. These may be due to large long-range static interactions which occur with the very high loading density of the polymers. It may also be due to the short flexible linkers in the main chain of the polymers. The short flexible linkers were designed to increase the site-isolation effect and T_g. However, they may cause large steric energy which hinders the chromophore rotation during the poling process. Further investigation is being undertaken to improve this approach.

Conclusion

Alternating polymers **P1** and **P2** of NLO chromophores and bulky spacers were synthesized. High chromophore loading and efficient site isolation were achieved using this approach. The alternating polymer can be poled to higher EO efficiency under a much lower poling field than the optimized guest−host system, while the λ_{max} of the polymer film is about 40 nm shorter than that of the guest−host system. Future work will focus on decreasing conductivity and increasing the length of the flexible linkers to achieve higher EO efficiency.

Experimental Section

General. All commercially available compounds were used as supplied unless noted in the procedures. THF was distilled over sodium under nitrogen before use. Pyridine was distilled over molecular sieves under nitrogen before use. All UV−visible spectra were recorded on a SHIMADZU

1601 UV spectrometer. ^{1}H and ^{13}C NMR spectra were recorded on Bruker AM 300 and AM 301 instruments. Differential scanning calorimetry were recorded on a SHIMADZU DSC-60. Elemental analysis was performed by Prevalere Life Sciences, Inc.

Synthetic Procedures. *Compound **5***. 5-Hydroxy-isophthalic acid dimethyl ester (1.41 g, 6.69 mmol) and potassium carbonate (1.11 g, 8.02 mmol) were dissolved with stirring in 15 mL of DMF. 1,3-Bis-benzyloxy-5-bromomethyl-benzene (2.05 g, 5.35 mmol) was added to the mixture which was then stirred under an argon atmosphere at room temperature for 24 h. Water (45 mL) was added to the mixture, and the organic phase was extracted with methylene chloride and dried over magnesium sulfate. After concentration under reduced pressure, the product was precipitated from methanol and collected by filtration and washing with methanol. The yield was 2.40 g (88%). ^{1}H NMR ($CDCl_3$): 3.96 (6H, s), 5.07 (4H, s), 5.10 (2H, s), 6.61 (1H t, $J = 2.3$ Hz), 6.71 (2H, d, $J = 2.3$ Hz), 7.4 (10H, m), 7.84 (2H, d, $J = 1.4$ Hz), 8.31 (1H, t, $J = 1.4$ Hz).

*Compound **3***. A solution of **5** (1 g, 1.95 mmol) in 50 mL of acetone was diluted with 28 mL of methanol. To the solution was added 9.5 mL of 1 N aqueous KOH solution. The resulting solution was stirred at room temperature for 24 h. The solution was then brought to a slightly acidic pH by slow addition of 5 N HCl solution. Organic solvents were removed by evaporation. The precipitate was collected by filtration and washed with water. The crude product was purified by a silica gel column using 10% methanol in methylene chloride as the eluent. The product was dried under high vacuum. Yield was 0.890 g (94%). ^{1}H NMR (DMSO): 5.09 (4H, s), 5.17 (2H, s), 6.64 (1H, t, $J = 2.2$ Hz), 6.74 (2H, d, $J = 2.3$ Hz), 7.38 (10H, m), 7.73 (2H, d, $J = 1.4$ Hz), 8.08 (1H, t, $J = 1.4$ Hz).

*Compound **6***. 5-Hydroxy-isophthalic acid dimethyl ester (1.08 g, 4.79 mmol) and K_2CO_3 (662 mg, 4.79 mmol) were dissolved in 15 mL of DMF. 1-Bromomethyl-2,3,4,5,6-pentafluoro-benzene (0.54 mL, 3.83 mmol) was then added to this mixture. The resulting mixture was stirred under an argon atmosphere at room temperature for 24 h. The reaction mixture was washed with 50 mL of water, and the organic phase was extracted with methylene chloride and dried over magnesium sulfate. After being concentrated under reduced pressure, the crude product was precipitated from methanol, collected by filtration, and then purified by a silica gel column using 5−10% ethyl acetate in hexanes as the eluent. The yield was 1.147 g (77%). ^{1}H NMR ($CDCl_3$): 3.98 (6H, s), 5.28 (2H, s), 7.86 (2H, d, $J = 1.4$ Hz), 8.39 (1H, t, $J = 1.4$ Hz).

*Compound **4***. Compound **6** (1.135 g, 2.91 mmol) was dissolved in 40 mL of methanol. KOH (0.85 g, 15.15 mmol) was added to the solution, and the resulting mixture was stirred at room temperature for 24 h. Water (1 mL) was added, and the reaction mixture was heated at 60 °C for 2.5 h. HCl (3 N) was added to the reaction mixture until an acidic pH was reached. The crude precipitate was collected by filtration, washed with water, and purified by being dissolved into a minimum amount of acetone and precipitated from diethyl ether. The yield was 0.85 g (78%). ^{1}H NMR (DMSO): 4.09 (3H, t, $J = 1.4$ Hz), 5.31 (2H, s), 7.76 (2H, d, $J = 1.4$ Hz), 8.13 (1H, t, $J = 1.4$ Hz). ^{13}C NMR (MeOD, proton decoupled): 57.87 (s), 61.43 (s), 108.05 (t, $J = 19.0$ Hz), 119.72 (s), 123.66 (s), 132.61 (s), 140.76 (dd, $J_1 = 244.2$ Hz, $J_2 = 23.6$ Hz), 143.12 (t, $J = 19$ Hz), 145.86 (dd, $J_1 = 244.2$ Hz, $J_2 = 23.6$ Hz), 158.32 (s), 167.03 (s). MS (ESP) *m*/*e*: 373.04 (M − H).

*Compound **2***. Compound **7** (4.0 g, 7.33 mmol) was dissolved in 40 mL of acetone. To this solution was added 5 mL of 6 N HCl(aq). After stirring for 4 h at room temperature, the mixture was neutralized by $NaHCO_3$. Most organic solvent was evaporated under reduced pressure. The precipitates were collected and washed with water. The crude product was dissolved in acetone and purified by a silica gel column using a solvent gradient beginning with ethyl acetate and finishing with 40% acetone in ethyl acetate as the eluent. The yield was 0.70 g (80%). ^{1}H NMR (acetone-d_6): 3.62 (4H, t, $J = 5.8$ Hz), 3.80 (4H, quartet, $J = 5.7$ Hz), 4.20 (2H, t, $J = 5.5$ Hz), 6.79 (2H, d, $J = 9.1$ Hz), 7.20 (2H, s), 7.24 (1H, d, $J = 4.04$ Hz), 7.46 (2H, d, $J = 9.1$ Hz), 7.82 (1H, d, $J = 3.9$ Hz) 9.87 (1H, s).

*Chromophore **1***. Compound **7** (0.2 g, 0.366 mmol) and 2-(3-cyano-4-methyl-5-phenyl-5-trifluoromethyl-5*H*-furan-2-ylidene)-malononitrile (0.15 g, 0.476 mmol) were dissolved in 0.6 mL of CH_2Cl_2. To this solution was added 3 mL of ethanol. After stirring overnight at room temperature, the precipitate was collected and purified by dissolving in a minimum amount of CH_2Cl_2 and precipitating from methanol. The yield was 0.28 g (91%). ^{1}H NMR ($CDCl_3$): 0.05 (12H, s), 0.91 (18H, s), 3.60 (4H, t, $J = 6.0$ Hz), 3.8 (4H, t, $J = 6.2$ Hz), 6.62 (1H, d, $J = 15.3$ Hz), 6.7 (2H, d, $J = 9.0$ Hz), 7.00 (1H, d, $J = 15.3$ Hz), 7.03 (1H, d, $J = 3.0$ Hz), 7.12 (1H, d, $J = 16$ Hz), 7.32 (1H, d, $J = 4.3$ Hz), 7.39 (2H, d, $J = 8.8$ Hz), 7.54 (5H, m), 7.81 (1H, d, $J = 15.3$ Hz). Anal. Calcd for $C_{45}H_{53}F_3N_4O_3SSi_2$: C, 64.10; H, 6.34; N, 6.64. Found: C, 64.09; H, 6.30; N, 6.71. UV−vis: ($CHCl_3$): $\lambda_{max} = 754$ nm.

*Polymer **3** (**P3**)*. Tosyl chloride (625 mg, 3.28 mmol) and *N*-piperidinoformamide (285 mg, 2.52 mmol) were dissolved in 2.4 mL of pyridine and stirred at room temperature for 30 min. Compound **3** (610 mg 1.26 mmol) was dissolved in 1.5 mL of pyridine. To this solution was added the tosyl chloride/*N*-piperidinoformamide solution. The resulting solution was first stirred at room temperature for 10 min, then placed in a 120 °C dimethyl silicone oil bath for 5 min, and then placed in an 80−90 °C oil bath for an additional 5 min. To this solution was then slowly added the solution of 400 mg (1.26 mmol) of **2** in 4 mL of pyridine over a period of 20 min while a 90 °C oil bath temperature was maintained. The resulting solution was stirred at 80−90 °C for 2.5 h. The product was precipitated by adding the solution to 300 mL of methanol dropwise. The crude product was dissolved in CH_2Cl_2 and precipitated from methanol. The yield was about 0.92 g. ^{1}H NMR ($CDCl_3$): 3.75 (4H, broad), 4.47 (4H, broad), 4.94 (6H, broad), 6.60 (3H, broad), 6.88 (5H, broad), 7.35 (13H, broad), 7.65 (2H, broad), 8.14 (1H, broad), 9.77 (1H, broad).

*Polymer **1** (**P1**)*. **P3** (400 mg) and 2-(3-cyano-4-methyl-5-phenyl-5-trifluoromethyl-5*H*-furan-2-ylidene)-malononi-

trile (400 mg, 1.27 mmol) were mixed with 2 mL of THF. To this solution was added a solution of 4 mg of ammonium acetate in 8 mL of ethanol, and it stirred at 70 °C for 2 h and at room temperature overnight. The precipitates were collected and added to 5 mL of CH_2Cl_2. This mixture was added to 150 mL of methanol through a plug of glass wool. The precipitates were collected and washed by methanol and ethanol. The yield was 502 mg. ^{1}H NMR ($CDCl_3$): 3.76 (4H, broad), 4.49 (4H, broad), 4.95 (6H, broad), 6.59 (4H, broad), 6.86 (5H, broad), 7.34 (13H, broad), 7.51 (5H, broad), 7.66 (3H, broad), 8.16 (1H, broad). T_g = 130 °C. UV−vis (CH_2Cl_2): λ_{max} = 691 nm. Anal. Calcd for $C_{62}H_{45}F_3N_4O_8S$: C, 69.98; H, 4.36; N, 5.27. Found: 69.19; H, 4.09; N, 5.28.

*Polymer **4** (**P4**).* **P4** was synthesized following a procedure similar to that of **P3**. ^{1}H NMR ($CDCl_3$): 3.84 (4H, broad), 4.09 (3H, broad), 4.55 (4H, broad), 5.04 (2H, broad), 6.94 (5H, broad), 7.35 (2H, broad), 7.64 (3H, broad), 8.17 (1H, broad), 9.81 (1H broad).

*Polymer **2** (**P2**).* **P2** was synthesized from **P3** following a procedure similar to that of **P1**. ^{1}H NMR ($CDCl_3$): 3.87 (4H, broad), 4.05 (3H, broad), 4.55 (4H, broad), 5.03 (2H, broad), 6.65 (1H, broad) 6.91 (5H, broad), 7.26 (2H, broad), 7.37 (1H, broad), 7.55 (5H, broad), 7.71 (3H, broad), 8.19 (1H, broad). T_g = 140 °C. UV−vis (CH_2Cl_2): λ_{max} = 690 nm. Anal. Calcd for $C_{49}H_{31}F_7N_4O_7S$: C, 61.70; H, 3.38; N, 5.87. Found: C, 60.75; H, 3.12; N, 5.62.

Acknowledgment. Support from the National Science Foundation, Air Force Office of Scientific Research, and Defense Advanced Research Projects Agency is gratefully acknowledged.

Supporting Information Available: UV−vis spectra of chromophore **1** and polymers **P1** and **P2** (PDF). This material is available free of charge via the Internet at http://pubs.acs.org.

CM0524392